



GLOBAL JOURNAL OF HUMAN SOCIAL SCIENCE
ARTS & HUMANITIES

Volume 12 Issue 15 Version 1.0 Year 2012

Type: Double Blind Peer Reviewed International Research Journal

Publisher: Global Journals Inc. (USA)

Online ISSN: 2249-460X & Print ISSN: 0975-587X

Pixel Purity Index Algorithm and n-Dimensional Visualization for ETM+ Image Analysis: A Case of District Vehari

By Farooq Ahmad & Qurat-ul-ain Fatima

University of the Punjab, New Campus, Lahore, Pakistan

Abstract - The hyperspectral image analysis technique, one of the most advanced remote sensing tools, has been used as a possible means of identifying from a single pixel or in the field of view of the sensor. An important problem in hyperspectral image processing is to decompose the mixed pixels into the information that contribute to the pixel, endmember, and a set of corresponding fractions of the spectral signature in the pixel, abundances, and this problem is known as un-mixing. The effectiveness of the hyperspectral image analysis technique used in this study lies in their ability to compare a pixel spectrum with the spectra of known pure vegetation, extracted from the spectral endmember selection procedures, including the reflectance calibration of Landsat ETM+ image using ENVI software, minimum noise fraction (MNF), pixel purity index (PPI), and n-dimensional visualization. The Endmember extraction is one of the most fundamental and crucial tasks in hyperspectral data exploitation, an ultimate goal of an endmember extraction algorithm is to find the purest form of spectrally distinct resource information of a scene.

Keywords : Algorithm, endmember, fraction, Landsat, MNF, n-dimension, PPI, remote sensing.

GJHSS-A Classification : FOR Code: 090905



Strictly as per the compliance and regulations of:



Pixel Purity Index Algorithm and n-Dimensional Visualization for ETM+ Image Analysis: A Case of District Vehari

Farooq Ahmad ^α & Qurat-ul-ain Fatima ^σ

Abstract - The hyperspectral image analysis technique, one of the most advanced remote sensing tools, has been used as a possible means of identifying from a single pixel or in the field of view of the sensor. An important problem in hyperspectral image processing is to decompose the mixed pixels into the information that contribute to the pixel, endmember, and a set of corresponding fractions of the spectral signature in the pixel, abundances, and this problem is known as un-mixing. The effectiveness of the hyperspectral image analysis technique used in this study lies in their ability to compare a pixel spectrum with the spectra of known pure vegetation, extracted from the spectral endmember selection procedures, including the reflectance calibration of Landsat ETM+ image using ENVI software, minimum noise fraction (MNF), pixel purity index (PPI), and n-dimensional visualization. The Endmember extraction is one of the most fundamental and crucial tasks in hyperspectral data exploitation, an ultimate goal of an endmember extraction algorithm is to find the purest form of spectrally distinct resource information of a scene. The endmember extraction tendency to the type of endmembers being derived, and the number of endmembers, estimated by an algorithm, with respect to the number of spectral bands, and the number of pixels being processed, also the required input data, and the kind of noise, if any, in the signal model surveying done. Results of the present study using the hyperspectral image analysis technique ascertain that Landsat ETM+ data can be used to generate valuable vegetative information for the District Vehari, Punjab Province, Pakistan.

Keywords : Algorithm, endmember, fraction, Landsat, MNF, n-dimension, PPI, remote sensing.

I. INTRODUCTION

The recent developments in remote sensing technology have witnessed two major trends in sensor improvement (Qiu et al., 2006). The hyperspectral imaging (Shippert, 2003) is concerned with the measurement, analysis, and interpretation of spectra acquired from a given scene at a short, medium or long distance by an airborne or satellite sensor (Goetz et al., 1985; Aspinall et al., 2002). The pixel purity index (González et al., 2010; Pal et al., 2011) allows for spatial data reduction. The pixels in the image that represent the 'most pure' spectral signatures are identified and subset from the mass majority of pixels

representing mixed pixels. A 'pure' pixel, also known as an endmember (Nascimento and Dias, 2005), can be envisioned as a homogenous area greater in spatial extent than the image pixel size, so that the recorded signal for that pixel represents a spectral profile for single surface information (Boardman, 1993; Boardman et al., 1995). It assumes that the pixel-to-pixel variability in a scene results from varying proportions of spectral endmembers (Rogge et al., 2007). The spectrum of a mixed pixel can be calculated as a linear combination of the endmember spectra weighted by the area coverage of each endmember within the pixel, if the scattering and absorption of electromagnetic radiation is derived from a single component on the surface (Keshava and Mustard, 2002; Rogge et al., 2007). Image endmembers are pixel spectra that lie at the vertices of the image simplex in n-dimensional space. Imagery may provide similarly meaningful endmembers that can be considered 'pure' or relatively 'pure' spectra, meaning that little or no mixing with other endmembers has occurred within a given pixel (Rogge et al., 2007). A mixed pixel is a picture element representing an area occupied by more than one ground cover type (Mozaffar et al., 2008). Spectral unmixing represents a significant step in the evolution of remote decompositional analysis that began with multispectral sensing (Shippert, 2003). It is a consequence of collecting data in greater and greater quantities and the desire to extract more detailed information about the resource composition (Keshava and Mustard, 2002). Spectral analysis extracts useful information might have missed otherwise from the raw pixel values of medium and high resolution imagery and can reveal hidden information locked in the pixels of imagery (Keshava and Mustard, 2002; Shippert, 2003).

The hyperspectral imagery provides opportunities to extract more detailed information than is possible using traditional multispectral data. The future of hyperspectral remote sensing is promising (Shippert, 2003). As newly commissioned hyperspectral sensors provide more imagery alternatives, and newly developed image processing algorithms provide more analytical tools, hyperspectral remote sensing is positioned to become one of the core technologies for geospatial research (Shippert, 2004), exploration, and monitoring.

Hyperspectral images have been used to detect soil properties including moisture, organic content, and

Author ^α : Department of Geography, University of the Punjab, New Campus, Lahore, Pakistan. E-mail : F.Ahmad@sheffield.ac.uk

Author ^σ : GIS Centre, PUCIT, University of the Punjab, Lahore, Pakistan.

salinity (Ben-Dor et al., 2002). Vegetation scientists have successfully used hyperspectral imagery to identify vegetation species (Clark and Swayze, 1995), study plant canopy chemistry (Aber and Martin, 1995; Shippert, 2003), and detect vegetation stress.

a) *Study Area*

The District Vehari (Figure 2 and 8) lies between 29° 36' and 30° 22' North latitude and 71° 44' and 72° 53' East longitude (GOP, 2000). The district is bounded on the north by and Khanewal and Sahiwal, on the east by Pakpattan, on the south by Bahawalpur and Bahawalnagar, on the west by Lodhran and Khanewal.

II. RESEARCH DESIGN AND METHODS

In this research paper Landsat ETM+ scene 2003 for the District Vehari (path 150, row 39) was used for hyperspectral image analysis. In order to use this scene, several steps were followed to prepare for an accurate extraction of vegetation endmember. These vital steps are: image registration, geometric correction, radiometric enhancement, and histogram equalization as discussed by Macleod and Congalton (1998), Mahmoodzadeh (2007) and Al-Awadhi et al., 2011. The scene was corrected and geo-referenced using projection UTM, zone 43 and datum WGS 84. Atmospheric correction operation was performed using ENVI software. Further, Minimum Noise Fraction (MNF), Pixel Purity Index (PPI), n-Dimensional Visualizer (n-DV) and Endmember Extraction technique has been used for hyperspectral image analysis (Figure 1).

The Pixel Purity Index (PPI) technique was adopted using ENVI 'automated spectral hourglass' application upon ETM+ image. The PPI was applied upon the full scene of the district. In this experiment 22,948,704 pixels were operated (Figure 3 and 4) using Automated Hourglass Parameters: Number of MNF bands to use: 6 (excluding Thermal IR and Panchromatic); Number of PPI Iterations: 5,000; PPI Threshold Value: 2.500; Maximum number of PPI Pixels to use for Endmember Selection: 10,000; and Mapping Methods were selected: Mixture Tuned Matched Filtering (MTMF), Spectral Angle Mapper (SAM), and Unmixing. The Endmembers were selected for processing flow, a series of tools that use the spectrally over-determined nature of hyperspectral data to find the most spectrally pure or spectrally unique pixels within the dataset. This set of endmember signatures (Bateson and Curtiss, 1996; Bateson et al., 2000) was then used in the full range of mapping algorithms available in ENVI to determine locations, and in some cases subpixel abundances of endmembers (Harris, 2006).

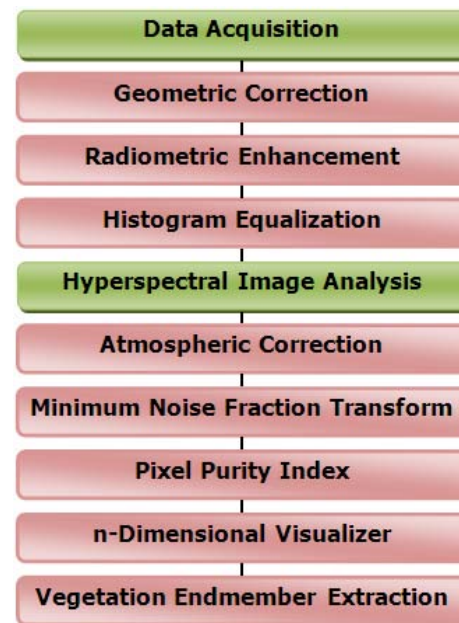


Figure 1 : Scheme for hyperspectral image analysis.

The hyperspectral imaging, also known as imaging spectrometry, is now a reasonably familiar concept in the world of remote sensing. Hyperspectral images are spectrally providing ample spectral information (Shippert, 2003) to identify and distinguish between spectrally similar resource information. Consequently, hyperspectral imagery provides the potential for more accurate and detailed information extraction than is possible with other types of remotely sensed data (Shippert, 2004). Standard multispectral image processing techniques were generally developed to classify multispectral images into broad categories of surface condition. Hyperspectral imagery provides an opportunity for more detailed image analysis. Boardman (1993) and Boardman et al. (1995) were among the first to develop and commercialize a sequence of algorithms specifically designed to extract detailed information from hyperspectral imagery (Shippert, 2004). ENVI tools, applicable to a variety of applications, distinguish and identify the unique resource information present in the scene and map them throughout the image (Research System, Inc., 2004).

III. RESULTS

The hyperspectral imaging is a new emerging technology in remote sensing which generates hundreds of images, at different wavelength channels, for the same area on the surface of the Earth (Goetz et al., 1985; González et al., 2010; Sánchez and Plaza, 2010). The concept of hyperspectral imaging originated at NASA's Jet Propulsion Laboratory in California, which developed instruments such as the Airborne Imaging Spectrometer (AIS), then called AVIRIS, for Airborne Visible Infrared Imaging Spectrometer (Green et al., 1998). This system is now able to cover the wavelength

region from 0.38 to 2.5 μm or 380 nm to 2500 nm using two hundred twenty four spectral channels, at nominal spectral resolution of 10 nm (González et al., 2010).

The Pixel Purity Index (PPI) is a new automated procedure in the hyperspectral analysis process (Boardman, 1993; Boardman et al., 1995) for defining potential image endmember spectra (Bateson and Curtiss, 1996) for spectral unmixing (Lillesand and Kiefer, 2000). When image spectra are treated as points in n-dimensional spectral space, endmember spectra should lie along the margins of the data cloud (Microlimages, Inc., 1999; Berman et al., 2004). The PPI creates a large number of randomly oriented test vectors anchored at the origin of the coordinate space. The spectral points are projected onto each test vector, and spectra within a threshold distance of the minimum and maximum projected values are flagged as extreme (Nascimento and Dias, 2005). As directions are tested, the process tallies the number of times an image cell is found to be extreme (Miao and Qi, 2007). Cells with high values in the resulting PPI raster should correspond primarily to 'edge' spectra (Chang et al., 2006). The PPI raster then can be used as a mask to control input to the n-dimensional visualizer (Microlimages, Inc., 1999; Zhang et al., 2008).

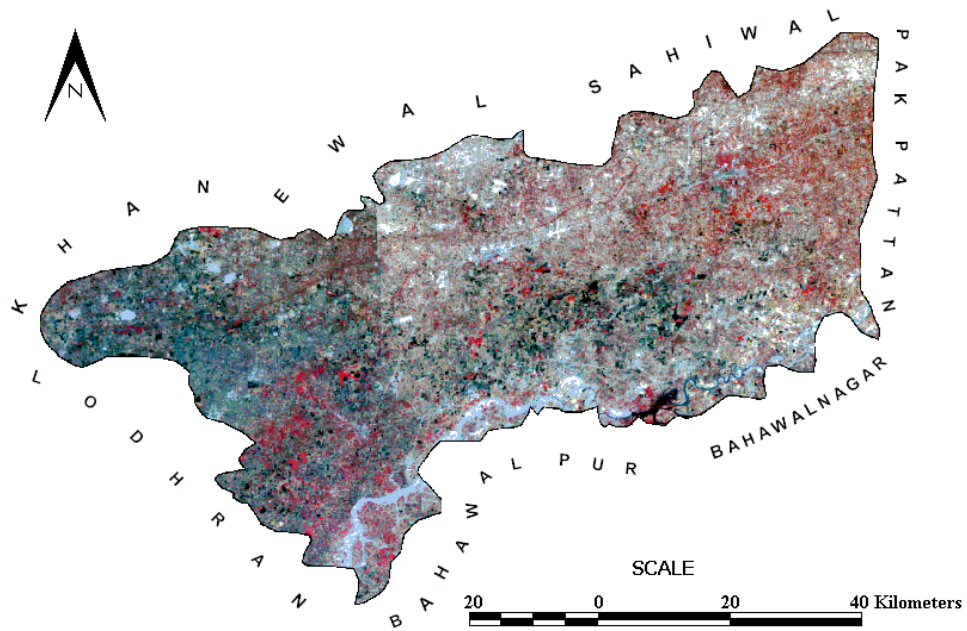
The most commonly used endmember extraction (Figure 5, 6 and Table 1, 2) tool is pixel purity index, which searches for vertices that define the data volume in n-dimensional space (Rogge et al., 2007). Commonly the first step of PPI is to apply MNF (Lee et al., 1990) to reduce the dimensionality of the data set (Green et al., 1988; Rogge et al., 2007). The MNF transform is used to determine the inherent dimensionality of image data, to segregate noise in the data, and to reduce the computational requirements for subsequent processing (Boardman and Kruse, 1994). The transformation based on an estimated noise covariance matrix, decorrelates and rescales the noise in the data (Research Systems, Inc., 2003; 2004). This step results in transformed data in which the noise has unit variance and no band-to-band correlations. For the purposes of further spectral processing, the inherent dimensionality of the data is determined by examination of the final eigenvalues and the associated images. The data space can be divided into two parts: one part associated with large eigenvalues and coherent eigenimages, and a complementary part with near-unity eigenvalues and noise-dominated images. By using only the coherent portions, the noise is separated from the data, thus improving spectral processing results (Research Systems, Inc., 2001; 2004).

Spectra can be thought of as points in an n-dimensional scatter plot, where n is the number of bands (Boardman et al., 1995). The coordinates of the points in n-space consist of 'n' values that are simply the spectral radiance or reflectance values in each band for a given pixel. The distribution of these points in n-space

can be used to estimate the number of spectral endmembers and their pure spectral signatures (Research Systems, Inc., 2001). The scatter plot (Figure 7) is an important tool for exploring an image and helping to understand some of the spectral characteristics of features in an image. The two dimensional scatter plotting tool allows comparing not only the relationship between the data values in two selected bands but also the spatial distribution in the image of pixels in any area of the scatter plot. This combined functionality provides a very simple, two-band, interactive classification of image data (Research Systems, Inc., 2004).

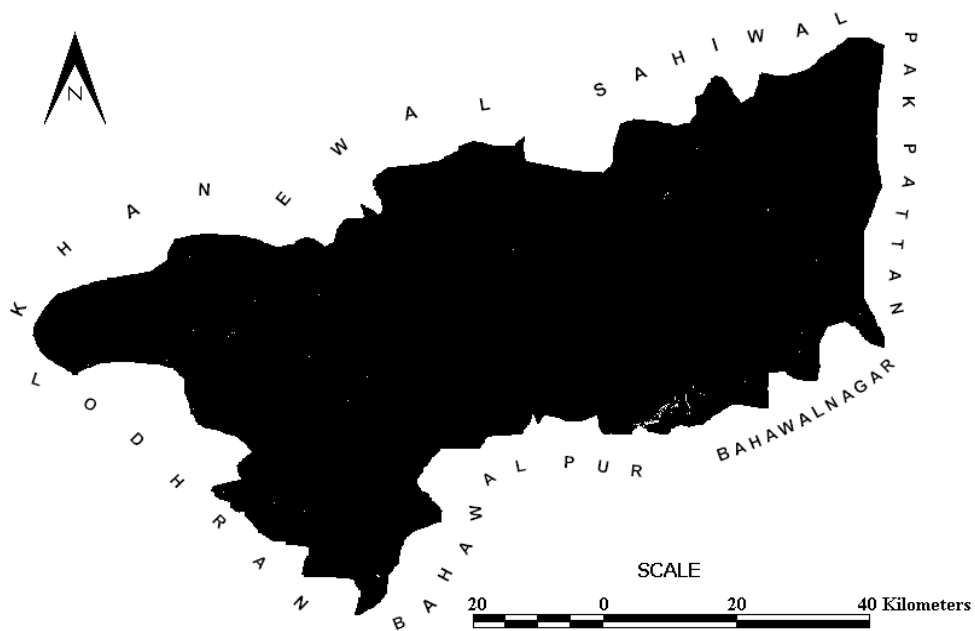
Spectral unmixing (Figure 9) algorithms (Lillesand and Kiefer, 2000; Rogge et al., 2006) use a variety of different statistical procedures to endmember extraction and estimate abundances. Unmixing problem comprises three sequential steps: dimension reduction, endmember determination, and inversion (Chang and Plaza, 2006). Because hyperspectral scenes can include extremely large amount of data, some algorithms for spectral unmixing first use image itself to estimate endmembers present in the scene. The dimension-reduction stage reduces the dimension of the original data in the scene (Cochrane, 2000; Mozaffar et al., 2008). The noise estimate can come from one of three sources; from the dark current image acquired with the data, from noise statistics calculated from the data (Richards and Jia, 1999), or from statistics saved from a previous transform. Both the eigenvalues and the Minimum Noise Fraction (MNF - Figure 10) images (eigenimages) are used to evaluate the dimensionality of the data (Qiu et al., 2006). Eigenvalues for bands that contain information will be an order of magnitude larger than those that contain only noise. The corresponding images will be spatially coherent, while the noise images will not contain any spatial information (Research Systems, Inc., 2004; Qiu et al., 2006).

Figure 2 : District Vehari - Landsat ETM+ 2003 image.



Source : <http://glovis.usgs.gov/> (Accessed on December 04, 2008) Processed by the author.

Figure 3 : Showing the endmember pixels extracted by the PPI for the District Vehari.



Processed by the author.



Table 1 : Showing selected endmembers data.

Bands	nD Class 1-2	nD Class 2-3	nD Class 3-4	nD Class 4-5	nD Class 5-6	nD Class 6-7	nD Class 7-8
1	81	74	75	84	74	76	76
2	68	62	62	84	61	64	66
3	78	66	67	99	69	74	75
4	70	57	68	77	71	86	64
5	255	103	255	48	255	255	109
8	1	255	255	38	1	1	255

Table 2 : Showing selected endmembers (MNF).

Bands	nD Class 1-2	nD Class 2-3	nD Class 3-4	nD Class 4-5	nD Class 5-6	nD Class 6-7	nD Class 7-8
1	-45.668144	-9.559686	-13.362324	-42.251820	-40.435787	-43.774044	-11.297052
2	-3.265855	-0.914537	18.957897	-11.722809	3.940382	14.638547	4.918655
3	15.752277	-29.919695	-23.210220	-2.429869	20.311623	26.381514	-31.349176
4	296.551239	-137.255051	52.496872	-22.368624	294.801758	282.927765	-135.733566
5	-27.440727	146.126907	160.149399	-48.182602	-19.783876	-24.758867	136.516922
6	139.244019	-62.703640	27.703362	1.272109	137.308945	129.952774	-63.861103

Figure 4 : Showing Pixel Purity Index Plot for the District Vehari.

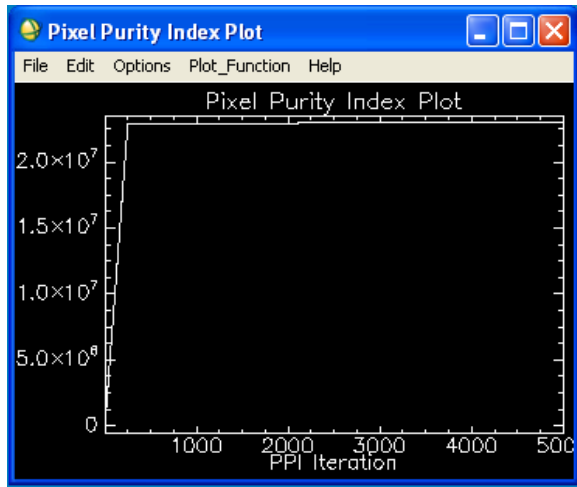


Figure 5 : Showing selected endmembers data.

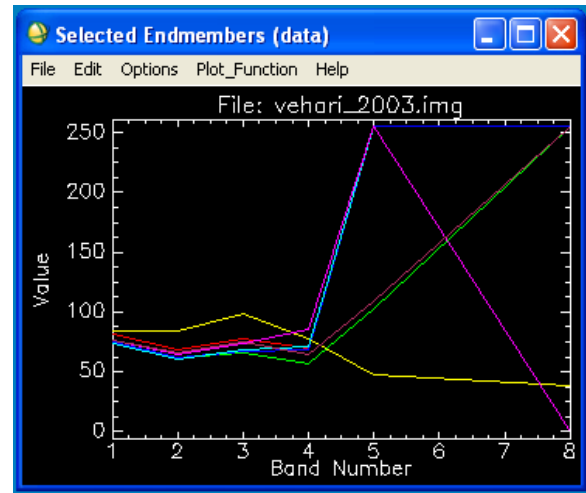


Figure 6 : Showing selected endmembers (MNF).

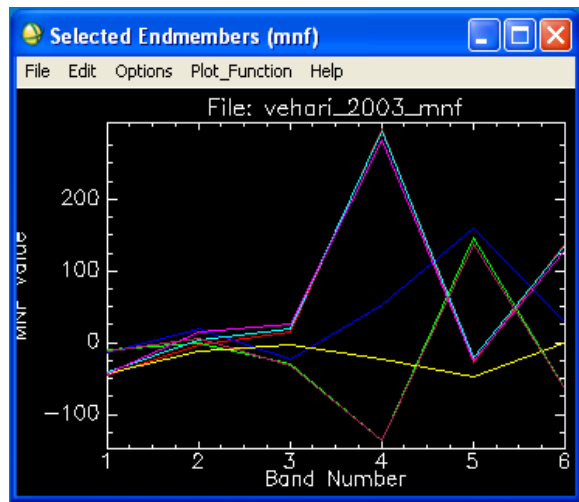
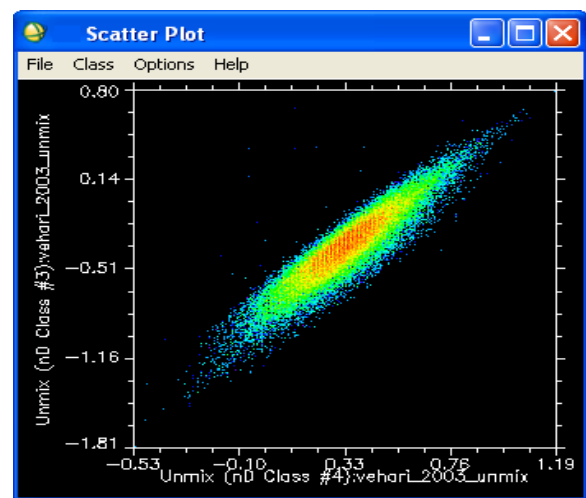


Figure 7 : 2-D scatter plot applied upon unmixing using band X 4 and band Y 3.



The Mixture Tuned Matched Filtering (MTMF - Figure 11) algorithm builds upon the strengths of both matched filtering and spectral unmixing while avoiding the disadvantages of both (Boardman, 1998). Matched filtering performs partial unmixing and identifies abundance of spectral endmembers without knowing background endmember signatures (Harsanyi and Chang 1994; Boardman et al., 1995). Matched filtering does not distinguish rare spectral targets very well and assumes an additive signal based upon radio/radar applications. Spectral unmixing takes advantage of the hyperspectral leverage to solve the linear mixed pixel problem, but traditional spectral unmixing techniques require knowledge of all of the background endmembers (Boardman, 1993; Bateson and Curtiss, 1996; Bateson et al., 2000). Incorporating convex geometry concepts, mixtures must be non-negative and unit-sum helps identify false positives, unrealistic mixtures, and maps subpixel fractional abundances.

The Minimum Noise Fraction (MNF) data reduction transform and Mixture Tuned Matched Filtering (MTMF) partial unmixing classification algorithm are relatively new image processing techniques that have proven to be effective target detection tools (Research Systems, Inc., 2004). These techniques allow partial unmixing and subpixel target abundance estimation, products that cannot be achieved using spectral angle mapping algorithms (Mundt et al., 2007).

The n-dimensional visualizer serves as an interactive tool for multidimensional analysis and identification of spectral endmembers (Tompkins et al., 1997; Plaza et al., 2002). The data are displayed in a defined number of dimensions and spectral

endmembers are identified as pixels that are located at the corner vertices (Tsai and Philpot, 1998). The n-dimensional visualizer second round of spatial data reduction designed to identify particular pixels or group of pixels that represent the purest spectra within the image. These pure spectra are exported and saved as ROI's that can be used for subsequent image classification techniques.

The n-dimensional visualizer was used to interactively locate, identify, and cluster the most spectrally pure or unique pixels in the image by visualizing those pixels selected from the PPI as points in a multidimensional scatter plot (Figure 7), where the number of dimensions was defined by the total number of coherent MNF bands (Boardman, 1993; Harris, 2006). The advantage of the n-dimensional visualizer was that it allowed visualization of points in an n-dimensional space, forming a data 'cloud' (Berk et al., 1998; Harris, 2006).

Advantages of this technology include both the qualitative benefits derived from a visual overview, and more importantly, the quantitative abilities for systematic assessment and monitoring (Shippert, 2003). A considerable number of mixed pixels are present in any remotely sensed image (Mozaffar et al., 2008). Several research objectives were accomplished :

- Select optimal bands in hyperspectral images those are most useful in vegetation classification,
- Identify optimal endmember, signature spectrum that represents a certain class, for vegetation classification, and
- Test effective endmember extraction algorithms for classification of vegetation type.

Figure 8 : Landsat ETM+, District Vehari.

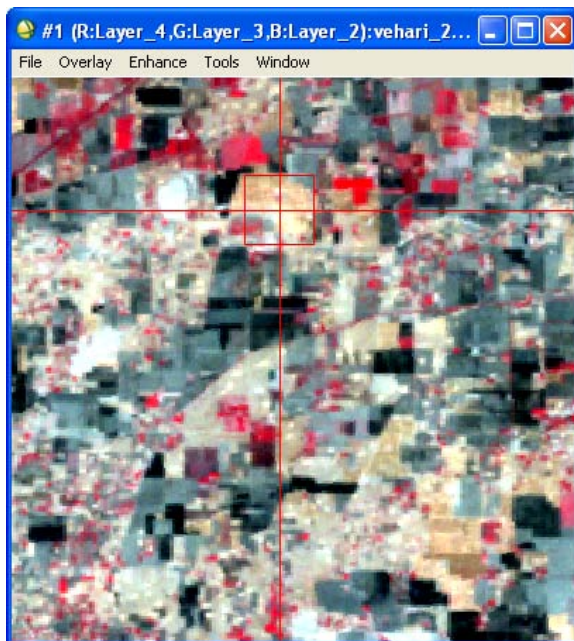


Figure 9 : Image showing unmixing.

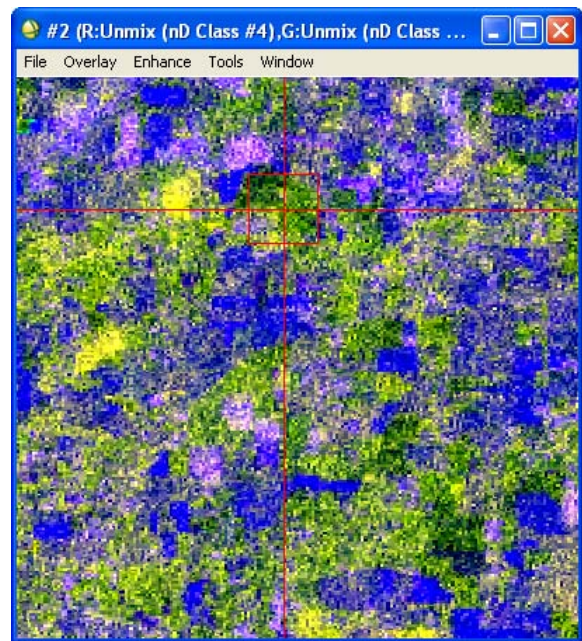


Figure 10 : Image showing minimum noise fraction (MNF).

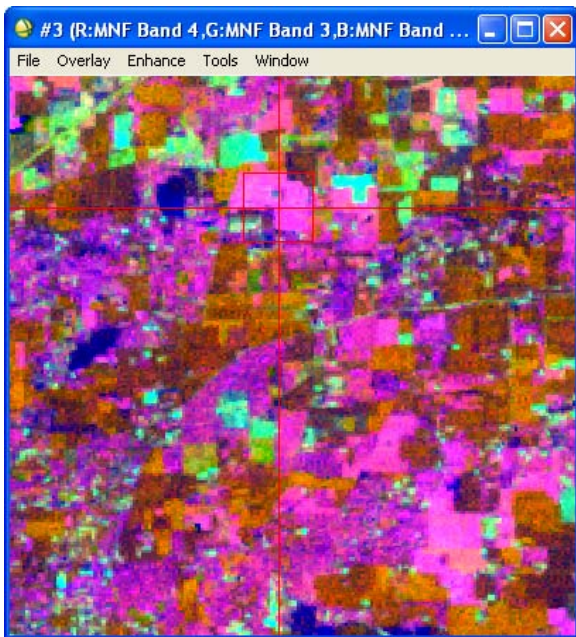
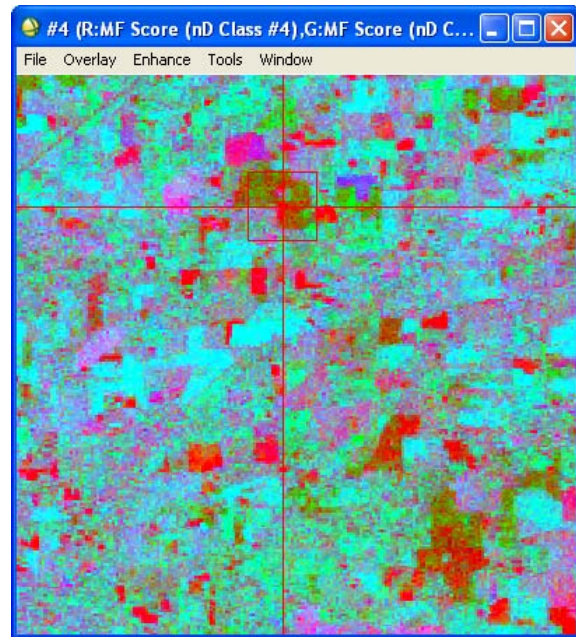


Figure 11 : Image showing mixture tuned matched filtering (MTMF).



IV. DISCUSSION AND CONCLUSIONS

The potential of hyperspectral remote sensing is exciting; there are special issues that arise with this unique type of imagery. For example, many hyperspectral analysis algorithms require accurate atmospheric corrections to be performed. To meet this need, sophisticated atmospheric correction algorithms have been developed to calculate concentrations of atmospheric gases directly from the detailed spectral information contained in the imagery (Roberts et al., 1993; Cochrane, 2000; Okin et al., 2001; Riano et al., 2002) itself without additional ancillary data. These corrections can be performed separately for each pixel because each pixel has a detailed spectrum associated with it. Several of these atmospheric correction algorithms are available within commercial image processing software (Shippert, 2004). However, several image analysis algorithms have been successfully used with uncorrected imagery (Shippert, 2003).

The MNF transform applied to the ETM+ data achieved a reasonable separation of coherent signal from complementary noise, therefore the MNF transformed eigenimages were employed and coupled with pixel purity index and n-dimensional visualization techniques to facilitate the extraction of the endmembers (Song, 2005; Qiu et al., 2006). After applying PPI thresholding, the data volume to be analyzed has been effectively reduced (Zhang et al., 2000). However, it is still possible that many less 'pure' pixels have crept in as candidate endmembers during the automatic selection process. All the pixels that were

previously selected using the PPI thresholding procedure are displayed as pixel clouds in the n-dimensional spectral space (Welch et al., 1998). To make possible the visualization of a scatter plot with more than two dimensions, the pixel clouds of high dimensions are cast on the two-dimensional display screen (Kruse et al., 1993; Tu et al., 1998). To effectively extract endmembers from high dimensional remote sensing data (Plaza et al., 2004) and to effectively process the data, it is often necessary that the dimensionality of the original data be decreased and noise in the data be segregated first, so the visualizing complexity and computational requirement for the subsequent analysis can be reduced (Kalluri et al., 2001; Qiu et al., 2006). This is often achieved through applying a minimum noise fraction transform to the high dimensional data (Qiu et al., 2006).

The hyperspectral sensors and analysis have provided more information from remotely sensed imagery than ever possible before. As new sensors provide more hyperspectral imagery and new image processing algorithms continue to be developed, hyperspectral imagery (Shippert, 2003) is positioned to become one of the most common research (Shippert, 2004), exploration, and monitoring technologies used in a wide variety of fields.

This paper has investigated the usage of ETM+ data for vegetation cover analysis of a semi-arid area in Pakistan. Landsat ETM+ data provide rich spectral information content. The open availability of Landsat data makes it attractive choice for many researchers in Pakistan. The hyperspectral image analysis technique

employed was implemented based on the comparison of a pixel spectrum with the spectra of known pure resource information, which can be effectively extracted using endmember selection procedures such as minimum noise fraction, pixel purity index and n-dimensional visualization.

V. ACKNOWLEDGEMENTS

The author wishes to thank his respected mentor Dr. Robert Bryant, Sheffield Centre for International Drylands Research, Department of Geography, The University of Sheffield for review and providing valuable comments on draft-version of this paper.

REFERENCES RÉFÉRENCES REFERENCIAS

- Aber JD and Martin ME (1995). High spectral resolution remote sensing of canopy chemistry, In: Summaries of the 5th Annual JPL Airborne Geoscience Workshop, pp.1-4. URL: ftp://popo.jpl.nasa.gov/pub/docs/workshops/95_docs/1.PDF. (Accessed on November 20, 2011).
- Al-Awadhi T, Al-Shukili A and Al-Amri Q (2011). The use of remote sensing & geographical information systems to identify vegetation: The case of Dhofar Governorate (Oman). URL: <http://www.isprs.org/proceedings/2011/ISRSE34/211104015Final00239.pdf>. (Assessed on September 10, 2011).
- Aspinall RJ, Marcus WA and Boardman JW (2002). Considerations in collecting, processing, and analyzing high spatial resolution hyperspectral data for environmental investigations. *Journal of Geographical Systems*, Vol. 4, pp.15-29.
- Bateson A and Curtiss B (1996). A method for manual endmember selection and spectral unmixing. *Remote Sensing of Environment*, Vol. 55, pp.229-243.
- Bateson A, Asner GP and Wessman CA (2000). Endmember bundles: A new approach to incorporating endmember variability into spectral mixture analysis, *IEEE Transactions on Geoscience and Remote Sensing*, Vol. 38(2), pp.1083-1094.
- Ben-Dor E, Patkin K, Banin A and Karnieli A (2002). Mapping of several soil properties using DAIS-7915 hyperspectral scanner data: A case study over clayey soils in Israel, *International Journal of Remote Sensing*, Vol. 23(6), pp.1043-1062. doi: 10.1080/01431160010006962.
- Berk A, Bernstein LS, Anderson GP, Acharya PK, Robertson DC, Chetwynd JH and Adler-Golden SM (1998). MODTRAN cloud and multiple scattering upgrades with application to AVIRIS, *Remote Sensing of Environment*, Vol. 65, pp.367-375.
- Berman M, Kiiveri H, Lagerstrom R, Ernst A, Dunne R and Huntington J (2004). ICE: An automated statistical approach to identifying endmembers in hyperspectral images, *IEEE Transactions on Geoscience and Remote Sensing*, Vol. 42, pp.2085-2095.
- Boardman JW (1993). Automating spectral unmixing of AVIRIS data using convex geometry concepts, In: Summaries of the 4th Annual JPL Airborne Geoscience Workshop, pp.11-14. URL: ftp://popo.jpl.nasa.gov/pub/docs/workshops/93_docs/4.PDF. (Accessed on November 19, 2011).
- Boardman JW (1998). Leveraging the high dimensionality of AVIRIS data for improved sub-pixel target unmixing and rejection of false positives: Mixture Tuned Matched Filtering, In: Summaries of the 7th Annual JPL Airborne Geoscience Workshop, p.6. URL: ftp://popo.jpl.nasa.gov/pub/docs/workshops/98_docs/8.pdf. (Accessed on November 28, 2011).
- Boardman JW and Kruse FA (1994). Automated spectral analysis: A geologic example using AVIRIS data, north Grapevine Mountains, Nevada, Proceedings of 10th Thematic Conference on Geologic Remote Sensing, Environmental Research Institute of Michigan, Ann Arbor, MI, Vol. 1, p.407 and p.418.
- Boardman JW, Kruse FA and Green RO (1995). Mapping target signatures via partial unmixing of AVIRIS data, In: Summaries of the 5th Annual JPL Airborne Geoscience Workshop, pp.23-26. URL: <http://trs-new.jpl.nasa.gov/dspace/bitstream/2014/33635/1/94-1613.pdf>. (Accessed on November 19, 2011).
- Chang CI and Plaza A (2006). A fast iterative algorithm for implementation of pixel purity index, *IEEE Geoscience and Remote Sensing Letters*, Vol. 3(1), pp.63-67. doi: 10.1109/LGRS.2005.856701
- Chang CI, Wu CC, Liu WW and Ouyang YC (2006). A new growing method for simplex-based endmember extraction algorithm, *IEEE Transactions on Geoscience and Remote Sensing*, Vol. 44, pp.2804-2819.
- Clark RN and Swayze GA (1995). Mapping minerals, amorphous materials, environmental materials, vegetation, water, ice, and snow, and other materials: The USGS Tricorder Algorithm, In: Summaries of the 5th Annual JPL Airborne Geoscience Workshop, pp.39-40. URL: <http://www.lpi.usra.edu/meetings/lpsc1995/pdf/1128.pdf>. (Accessed on November 20, 2011).
- Cochrane MA (2000). Using vegetation reflectance variability for species level classification of hyperspectral data, *International Journal of Remote Sensing*, Vol. 21(10), pp.2075-2087.
- Goetz AFH, Vane G, Solomon JE and Rock BN (1985). Imaging spectrometry for Earth remote sensing, *Science*, Vol. 228(4704), pp.1147-1153. doi: 10.1126/science.228.4704.1147.
- González C, Resano J, Mozos D, Plaza A and Valencia D (2010). FPGA implementation of the pixel

- purity index algorithm for remotely sensed hyperspectral image analysis, *EURASIP Journal on Advances in Signal Processing*, Vol. 2010, pp.1-13. doi: 10.1155/2010/969806.
19. GOP (2000). District census report of Vehari 1998, Population Census Organization, Statistics Division, Government of Pakistan, Islamabad, Pakistan, p.1.
 20. Green AA, Berman M, Switzer P and Craig MD (1988). A transformation for ordering multispectral data in terms of image quality with implications for noise removal, *IEEE Transactions on Geoscience and Remote Sensing*, Vol. 26, pp.65-74.
 21. Green RO, Eastwood ML and Sarture CM (1998). Imaging spectroscopy and the airborne visible/infrared imaging spectrometer (AVIRIS), *Remote Sensing of Environment*, Vol. 65(3), pp.227-248.
 22. Harris AT (2006). Spectral mapping tools from the earth sciences applied to spectral microscopy data, *Cytometry, Part A* 69A, pp.872-879. doi: 10.1002/cyto.a.
 23. Harsanyi JC and Chang CI (1994). Hyperspectral image classification and dimensionality reduction: An orthogonal subspace projection approach, *IEEE Transactions on Geoscience and Remote Sensing*, Vol. 32, pp.779-785.
 24. Kalluri S, Zhang Z, JaJa J, Liang S and Townshend J (2001). Characterizing land surface anisotropy from AVHRR data at a Global scale using high performance computing, *International Journal of Remote Sensing*, Vol. 22, pp.2171-2191.
 25. Keshava N and Mustard JF (2002). Spectral unmixing, *IEEE Signal Processing Magazine*, Vol. 19(1), pp.44-57. doi: 10.1109/79.974727.
 26. Kruse FA, Lefkoff AB, Boardman JW, Heidebrecht KB, Shapiro AT, Barloon PJ and Goetz AFH (1993). The spectral image processing system (SIPS) interactive visualization and analysis of imaging spectrometer data, *Remote Sensing of Environment*, Vol. 44, pp.145-163.
 27. Lee JB, Woodyatt S and Berman M (1990). Enhancement of high spectral resolution remote sensing data by a noise-adjusted principal components transform, *IEEE Transactions on Geoscience and Remote Sensing*, Vol. 28(3), pp.295-304.
 28. Lillesand TM and Kiefer RW (2000). *Remote sensing and image interpretation*, 4th Edition, John Wiley & Sons, Inc., New York, pp.178-198.
 29. Macleod RD and Congalton RG (1998). A quantitative comparison of change detection algorithms for monitoring eelgrass from remotely sensed data, *Photogrammetric Engineering & Remote Sensing*, Vol. 64(3), pp.207-216.
 30. Mahmoodzadeh H (2007). Digital change detection using remotely sensed data for monitoring green space destruction in Tabriz, *International Journal of Environmental Research*, Vol. 1(1), pp.35-41.
 31. Miao L and Qi H (2007). Endmember extraction from highly mixed data using minimum volume constrained nonnegative matrix factorization, *IEEE Transactions on Geoscience and Remote Sensing*, Vol. 45, pp.765-777.
 32. MicroImages, Inc (1999). Pixel purity index and masking aid endmember selection, TNTmips V6.10. URL: <http://www.microimages.com/documentation/TechGuides/61Ppi.pdf>. (Accessed on November 28, 2011).
 33. Mozaffar MH, Zoj MJV, Sahebi MR and Rezaei Y (2008). Vegetation endmember extraction in Hyperion images, URL: www.isprs.org/proceedings/XXXVII/congress/7_pdf/3.../34.pdf. (Accessed on November 20, 2011).
 34. Mundt JT, Streutker DR and Glenn NF (2007). Partial unmixing of hyperspectral imagery: Theory and methods, Paper in ASPRS Annual Conference, May 7-11, 2007, Tampa, Florida. URL <http://www.asprs.org/a/publications/proceedings/taempa2007/0046.pdf>. (Accessed on November 28, 2011).
 35. Nascimento JMP and Dias JMB (2005). Vertex component analysis: A fast algorithm to unmix hyperspectral data, *IEEE Transactions on Geoscience and Remote Sensing*, Vol. 43(4), pp.898-910. doi: 10.1109/TGRS.2005.844293.
 36. Okin GS, Roberts DA, Burray B and Okin WJ (2001). Practical limits on hyperspectral vegetation discrimination in arid and semiarid environments, *Remote Sensing of Environment*, Vol. 77, pp.212-225.
 37. Pal SK, Majumdar TJ, Bhattacharya AK and Bhattacharyya R (2011). Utilization of Landsat ETM+ data for mineral-occurrences mapping over Dalma and Dhanjori, Jharkhand, India: An advanced spectral analysis approach, *International Journal of Remote Sensing*, Vol. 32(14), pp.4023-4040.
 38. Plaza A, Martinez P, Perez R and Plaza J (2002). Spatial/spectral endmember extraction by multidimensional morphological operations, *IEEE Transactions on Geoscience and Remote Sensing*, Vol. 40, pp.2025-2041.
 39. Plaza A, Martinez P, Perez R and Plaza J (2004). A quantitative and comparative analysis of endmember extraction algorithms from hyperspectral data, *IEEE Transactions on Geoscience and Remote Sensing*, Vol. 42(3), pp.650-663.
 40. Qiu F, Abdelsalam M and Thakkar P (2006). Spectral analysis of ASTER data covering part of the Neoproterozoic Allaqi-Heiani suture, Southern Egypt, *Journal of African Earth Sciences*, Vol. 44, pp.169-180.
 41. Research System, Inc (2004). Exploring ENVI, Boulder, CO. URL: <http://www.ittvis.com> (Accessed on November 28, 2011).

42. Research Systems, Inc (2001). ENVI user's guide, Research Systems, Boulder, CO. URL: <http://www.ittvis.com> (Accessed on November 17, 2011).
43. Research Systems, Inc (2003). ENVI Tutorial: Advanced hyperspectral analysis, Boulder, CO. URL: <http://www.ittvis.com> (Accessed on November 20, 2011).
44. Riano D, Chuvieco E, Ustin S, Zomer R, Dennison P, Roberts D and Salas J (2002). Assessment of vegetation regeneration after fire through multitemporal analysis of AVIRIS image in the Santa Monica Mountains, Remote Sensing of Environment, Vol. 79, pp.60-71.
45. Richards JA and Jia X (1999). Remote sensing digital image analysis: An Introduction, Third Edition, Springer-Verlag, Berlin, pp.138-153.
46. Roberts DA, Smith MO and Adams JB (1993). Green vegetation, non-photosynthetic vegetation, and soils in AVIRIS data, Remote Sensing of Environment, Vol. 44, pp.255-269.
47. Rogge DM, Rivard B, Zhang J and Feng J (2006). Iterative spectral unmixing for optimizing per-pixel endmember sets, IEEE Transactions on Geoscience and Remote Sensing, Vol. 44, pp.3725-3736.
48. Rogge DM, Rivard B, Zhang J, Sanchez A, Harris J and Feng J (2007). Integration of spatial-spectral information for the improved extraction of endmembers, Remote Sensing of Environment, Vol. 110, pp.287-303.
49. Sánchez S and Plaza A (2010). GPU implementation of the pixel purity index algorithm for hyperspectral image analysis. URL: <http://www.umbc.edu/rssi/pl/people/aplaza/Papers/Conferences/2010.Cluster.GP.U.pdf>. (Accessed on November 20, 2011).
50. Shippert P (2003). Introduction to hyperspectral Communication, Issue 3. URL: <http://spacejournal.ohio.edu/pdf/shippert.pdf>. (Accessed on November 20, 2011).
51. Shippert P (2004). Why use hyperspectral imagery? Photogrammetric Engineering & Remote Sensing, pp.377-380. URL: <http://www.iro.umontreal.ca/~mignotte/IFT6150/ComplementCours/HyperspectralallImagery.pdf>. (Accessed on November 20, 2011).
52. Song C (2005). Spectral mixture analysis for subpixel vegetation fractions in the urban environment: How to incorporate endmember variability, Remote Sensing of Environment, Vol. 95, pp.248-263.
53. Tompkins S, Mustard JF, Pieters CM and Forsyth DW (1997). Optimization of endmembers for spectral mixture analysis, Remote Sensing of Environment, Vol. 59, pp.472-489.
54. Tsai F and Philpot W (1998). Derivative analysis of hyperspectral data, Remote Sensing of Environment, Vol. 66, pp.41-51.
55. Tu T, Chen C and Chang C (1998). A noise subspace projection approach to target signature detection and extraction in an unknown background for hyperspectral images, IEEE Transactions on Geoscience and Remote Sensing, Vol. 36(1), pp.171-181.
56. USGS (2008). Earth Resources Observation and Science Center. URL: <http://glovis.usgs.gov/> (Accessed on December 04, 2008).
57. Welch R, Jordan T, Lang H and Murakami H (1998). ASTER as a source for topographic data in the late 1990's, IEEE Transactions on Geoscience and Remote Sensing, Vol. 36, pp.1282-1289.
58. Zhang B, Wang X, Liu J, Zheng L and Tong Q (2000). Hyperspectral image processing and analysis system (HIPAS) and its applications, Photogrammetric Engineering & Remote Sensing, Vol. 66, pp.605-609.
59. Zhang J, Rivard B and Rogge DM (2008). The successive projection algorithm (SPA), an algorithm with a spatial constraint for the automatic search of endmembers in hyperspectral data, Sensors, Vol. 8, pp.1321-1342.